Simultaneous description of hadron and jet suppression in heavy-ion collisions

J. Casalderrey-Solana,[1,2] Z. Hulcher,[3] G. Milhano,[4,5] D. Pablos,[6,7] and K. Rajagopal[8]

[1]*Departament de Física Quàntica i Astrofísica & Institut de Ciències del Cosmos (ICC), Universitat de Barcelona,
Martí i Franquès 1, 08028 Barcelona, Spain*

[2]*Rudolf Peierls Centre for Theoretical Physics, University of Oxford, Clarendon Laboratory, Parks Road Oxford OX1 3PU, United Kingdom*

[3]*Cavendish Laboratory, University of Cambridge, JJ Thomson Avenue, Cambridge CB3 0HE, United Kingdom*

[4]*LIP, Avenida Prof. Gama Pinto, 2, P-1649-003 Lisboa, Portugal*

[5]*Instituto Superior Técnico (IST), Universidade de Lisboa, Avenida Rovisco Pais 1, 1049-001, Lisbon, Portugal*

[6]*Department of Physics, McGill University, 3600 University Street, Montréal, QC, H3A 2T8, Canada*

[7]*Department of Physics and Astronomy, Wayne State University, Detroit, Michigan 48201, USA*

[8]*Center for Theoretical Physics, Massachusetts Institute of Technology, Cambridge, Massachusetts 02139, USA*

We present a global fit to all data on the suppression of high-energy jets and high-energy hadrons in the most central heavy-ion collisions at the CERN Large Hadron Collider (LHC) for two different collision energies, within a hybrid strong-weak coupling quenching model. Even though the measured suppression factors for hadrons and jets differ significantly from one another and appear to asymptote to different values in the high-energy limit, we obtain a simultaneous description of all these data after constraining the value of a single model parameter. We use our model to investigate the origin of the difference between the observed suppression of jets and hadrons and relate it, quantitatively, to the observed modification of the jet fragmentation function in jets that have been modified by passage through the medium produced in heavy-ion collisions. In particular, the observed increase in the fraction of hard fragments in medium-modified jets, which indicates that jets with the fewest hardest fragments lose the least energy, corresponds quantitatively to the observed difference between the suppression of hadrons and jets. We argue that a harder fragmentation pattern for jets with a given energy after quenching is a generic feature of any mechanism for the interaction between jets and the medium that they traverse that yields a larger suppression for wider jets. We also compare the results of our global fit to LHC data to measurements of the suppression of high-energy hadrons in BNL Relativistic Heavy Ion Collider (RHIC) collisions, and find that with its parameter chosen to fit the LHC data, our model is inconsistent with the RHIC data at the 3σ level, suggesting that hard probes interact more strongly with the less hot quark-gluon plasma produced at RHIC.

Introduction. One of the most striking observations of the heavy-ion physics programs of both the BNL Relativistic Heavy Ion Collider (RHIC) and the CERN Large Hadron Collider (LHC) is the suppression in the measured yield of high-energy jets and hadrons in ultrarelativistic nucleus-nucleus collisions relative to the yield from an incoherent superposition of independent nucleon-nucleon collisions. This phenomenon is a direct consequence of the energy loss experienced by the high-energy partons that form jets and subsequently decay into hadrons as these partons traverse the strongly coupled quark-gluon plasma (QGP) produced in the same heavy-ion collisions. Since such parton-medium interactions have the potential to provide tomographic information about the microscopic properties of QGP, the suppression patterns of different energetic probes have been the subject of considerable experimental and theoretical research. For reviews, see Refs. [1–4].

One of the important questions posed by today's data is how to understand the basic empirical feature that high-energy hadrons are less suppressed than jets with the same or higher energies. We use an analysis couched within a specific model for jet quenching to elucidate a generic explanation for this characteristic feature of the observed data. In doing so, we find evidence in support of generic aspects of the parton-medium interaction responsible for jet quenching that are necessary to explain the observed systematics.

Jets are the sprays of hadrons produced as partons from a hard collision fragment into showers of partons which ultimately become hadrons. As the energetic partons that form jets traverse the QGP, they lose energy, and the properties of the resulting jets are modified. Because the production rate for jets in elementary collisions drops rapidly with increasing jet energy, jet energy loss implies a suppression in the yield of jets with a given energy relative to what it would have been

in the absence of any medium. Since high-energy hadrons originate from partons within jets, this suppression in turn translates into the suppression of high-energy hadrons. While the suppression pattern of jets and hadrons are therefore related to each other, even in LHC heavy-ion collisions with the highest center of mass energy per nucleon pair achieved to date, $\sqrt{s_{NN}} = 5.02$ TeV, the production of jets with a given energy is more suppressed than the production of hadrons with the same energy, and, it seems, the production of the highest energy jets that have been measured is more suppressed than the production of the highest energy hadrons that have been measured [5–7]. We provide an explanation of these basic systematic features in the data.

The essence of our explanation originates from the fact that when one selects a hadron with a specified high p_T, although this hadron originates from a jet the population of jets that is selected in this way is not typical, not representative of the generic population of jets selected calorimetrically by finding sprays of particles whose total p_T has a specified value. In particular, the population of jets that dominate the production of high-p_T hadrons will have a nongeneric probability distribution for their angular widths, as we now explain. The fact that the jet spectrum is steeply falling as a function of p_T^{jet} means that a hadron with any given large p_T^{hadron} is most likely to be a hadron that carries a large fraction of all the energy of the jet in which it finds itself. This is because if the hadron carried a smaller fraction of the total energy of its jet, that would mean its jet had a larger total p_T^{jet}, which is less likely because the spectrum is steeply falling. Consequently, high-energy hadrons belong to an unrepresentative subset of jets which happen to fragment such that they contain very few hard partons outside the jet core, and are consequently narrow in their angular extent. If jets of this type lose less energy than typical jets, this explains why the yield of high-p_T hadrons is less suppressed than the yield of high-p_T jets. Furthermore, if wider jets that contain more partons at large angles lose more energy due to quenching, this together with the steeply falling jet spectrum means that quenching makes it more likely to find, at any fixed p_T, narrow jets with fewer harder hadrons, since they are the ones that lost less energy. So, the same physics that explains why hadrons are more suppressed than jets also yields a modification, namely, a hardening, of the jet fragmentation function.

There are many extant models for the jet-medium interaction in which hard fragmenting, narrow, jets lose less energy than typical, wider, jets. Examples include models based entirely on perturbative QCD [8], strong coupling models built entirely using holographic techniques [9,10], and the hybrid model that we shall employ [11–14]. Within the hybrid model, we shall show that the same physics which enhances the probability for finding hard fragments in jets that have traversed a droplet of plasma explains the observed difference between the suppression of hadrons and jets. We argue that this should be the case, at least qualitatively, in any model with the feature that narrow jets lose less energy than wide jets.

Hybrid strong-weak coupling model. The physics of hard parton production and subsequent showering can be analyzed perturbatively, with weakly coupled QCD, making it natural

to develop weakly coupled analyses of parton energy loss in medium [1,2,15–43]. A weakly coupled calculation is, however, not the natural starting point with which to describe the hydrodynamic expansion of the droplets of strongly coupled QGP produced in RHIC and LHC collisions, and may not be the best starting point for describing the physics of typical soft momentum exchanges between partons in a jet shower and this medium. Complementarily, numerous qualitative insights into the properties of the strongly coupled QGP can be obtained from gauge-gravity duality, which has emerged as a tool with which to analyze the dynamics of droplets of strongly coupled gauge theory plasmas that are similar to QGP. (See Ref. [44] for a review.) These methods cannot be employed to describe hard processes, such as jet production, which are sensitive to short-distance physics where QCD *is* weakly coupled. The wide range of physical scales in play make the understanding of jet and hadron suppression an interesting theoretical challenge.

To address this challenge, a phenomenological hybrid model that exploits the separation between jet and medium scales and brings together the relevant description of physics at each energy scale was developed in Refs. [11–14]. In the model, partons generated in a hard collision, whose production is well described by diagrammatic techniques in perturbative QCD, relax their virtuality Q down to the hadronization scale Λ_{QCD} through successive splittings, following Dokshitzer-Gribov-Lipatov-Altarelli-Parisi (DGLAP) evolution equations as implemented in PYTHIA. Given that throughout most of the showering process, $Q \gg T$, with T the medium temperature, we leave the splittings within the shower unmodified. Simultaneous with the splitting processes, the partons in the developing shower traverse an expanding cooling droplet of QGP, and since $T \sim \Lambda_{\mathrm{QCD}}$, we must treat their interactions with the medium in which they find themselves nonperturbatively. This motivates modeling the energy degradation of the partons in the jet shower by applying geometric intuition from holography. Via gauge-gravity duality, the energy loss of a quark traveling through hot $\mathcal{N} = 4$ supersymmetric Yang-Mills (SYM) plasma at infinite coupling and large N_c is given by [45,46]

$$\left.\frac{dE}{dx}\right|_{\mathrm{strongly\ coupled}} = -\frac{4}{\pi} E_{\mathrm{in}} \frac{x^2}{x_{\mathrm{therm}}^2} \frac{1}{\sqrt{x_{\mathrm{therm}}^2 - x^2}} \quad , \quad (1)$$

where E_{in} is the parton's initial energy, and $x_{\mathrm{therm}} = (E_{\mathrm{in}}^{1/3}/T^{4/3})/2\kappa_{\mathrm{sc}}$ is the maximum distance that a parton with this energy can travel through the strongly coupled plasma. The "lost" energy and momentum become part of the droplet of QGP, generating a wake therein that will follow a hydrodynamic evolution, eventually decaying into soft hadrons that, by momentum conservation, carry the lost momentum in the direction of the original jet [13]. While in $\mathcal{N} = 4$ SYM the value of $\kappa_{\mathrm{sc}} \approx 1$ has been determined, its value must be less in the QGP of QCD which has fewer degrees of freedom. One of the assumptions of the hybrid model [11,12] is that all the differences between the interactions of jets with this strongly coupled plasma and the QGP of QCD can be accounted for by varying this parameter. In this way, κ_{sc} becomes the principal

free parameter in the model, controlling the degree of parton energy loss. We shall determine its value by fitting to data.

Despite its simplicity, this hybrid strong-weak coupling model has been very successful at describing and predicting inclusive jet and dijet observables [11], photon-jet and Z^0-jet observables [12], as well as the more differential jet sub- and superstructure observables [13]. In Ref. [14], the model was extended to incorporate the fact that plasma cannot resolve the internal structure of a parton shower with arbitrary precision, but can only interact independently with distinct excitations if they are separated by more than the plasma resolution length L_{res}. While this is a well-studied phenomenon occurring both at weak [47–50] and strong coupling [51], the analysis in Ref. [14] is the first exploratory study of these effects within a jet-quenching Monte Carlo. Here, we do our global fit for $L_{\text{res}} = 0$ and for the reasonable (see Ref. [14]) value $L_{\text{res}} = 2/(\pi T)$.

Fit to hadron and jet suppression data. We fix the free parameter of the model, κ_{sc}, by fitting to hadron and jet data from LHC collisions (PbPb collisions at $\sqrt{s_{NN}} = 2.76$ [52–55] and 5.02 TeV [5–7] in the most central bins). The simulations rely on the event generator PYTHIA 8.230 [56] for the production and DGLAP evolution of the shower, and we include leading-order nuclear parton distribution functions as parametrized in Ref. [57]. The space-time picture of the shower is built by assuming that the effective lifetime of each parton corresponds to $\tau = 2E/Q^2$, with E and Q the energy and virtuality of that parton, respectively [11,58]. When we choose $L_{\text{res}} = 2/(\pi T)$ instead of $L_{\text{res}} = 0$, this effectively delays these splitting times by delaying the time at which the QGP resolves a newly split pair of partons [14]. The local temperature and fluid velocity of the QGP needed to compute parton energy loss are read from hydrodynamic profiles for droplets of expanding cooling plasma that yield good descriptions of soft observables such as particle multiplicity and flow coefficients [59]. These hydrodynamic simulations have a starting time of $\tau_0 = 0.6$ fm, before which we assume there is no energy loss. As in Refs. [11–14], we do all calculations for two different values of the temperature, $T_c = 145$ and 170 MeV, below which we stop applying energy loss. This provides a crude proxy to the sensitivity to some systematic effects not included in the model. In order to estimate the contribution to the final hadron spectra coming from the wake generated by the passage of the jet through the plasma, as in Ref. [13] we assume that the wake hydrodynamizes subject to momentum conservation, becomes a small perturbation to the bulk hydrodynamic flow, and yields a correction to the final hadron spectrum (obtained via the Cooper-Frye prescription [60]), which is also a small perturbation that can be linearized. We perform the hadronization of the parton shower using the Lund string model present in PYTHIA without modification of color flows.

The six panels of Fig. 1 show the results for the fits to the best values of κ_{sc} for the two different values of T_c (first three panels for $T_c = 145$ MeV, last three for $T_c = 170$ MeV), and for $L_{\text{res}} = 0$ and $2/(\pi T)$. The fits have been done in two different ways. First, the individual points with error bars are obtained by fitting the model, separately, to each of ten different sets of data using a standard χ^2 analysis with
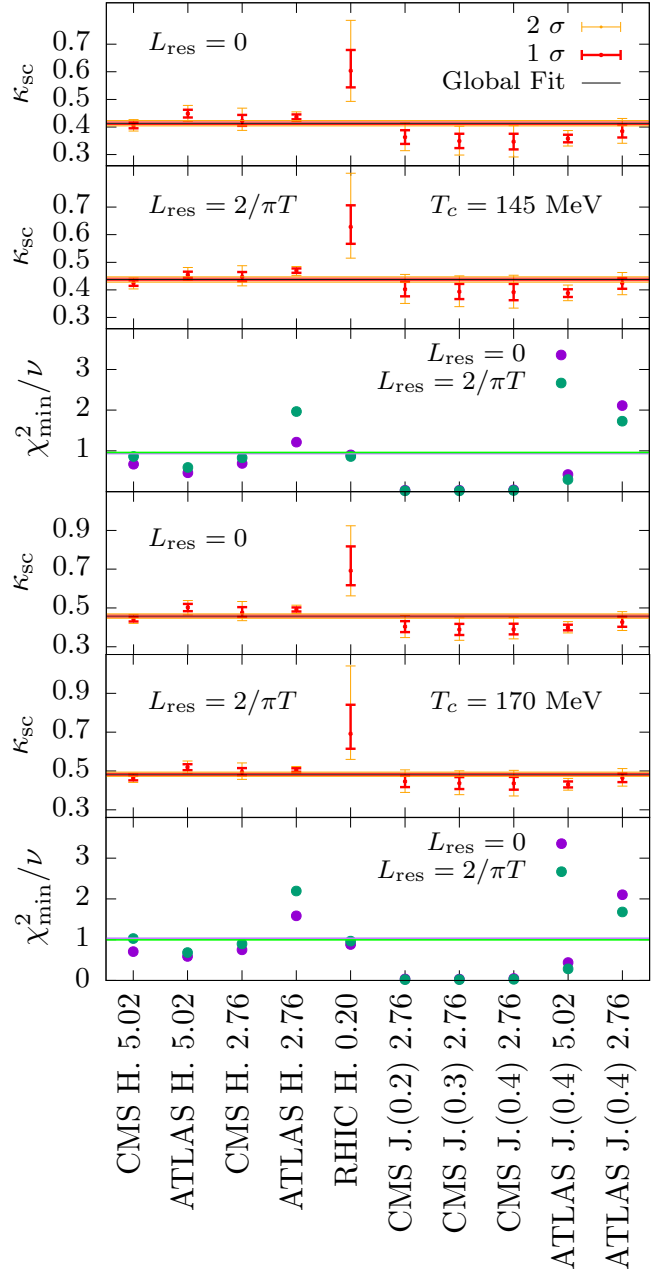

FIG. 1. Best values of κ_{sc} for $T_c = 145$ MeV (first three panels) and 170 MeV (last three panels). The individual red (orange) error bars show the 1σ (2σ) uncertainties in the value of κ_{sc} obtained by fitting separately to each one of ten data sets, nine from the LHC and one from RHIC. "H" stands for charged hadrons (LHC, PbPb collisions, $\sqrt{s_{NN}}$ specified in TeV) or π^0 (PHENIX, AuAu collisions, $\sqrt{s_{NN}}$ again specified in TeV) in the 0–5% centrality bin, while "J" stands for calorimetrically reconstructed jets, with the anti-k_t radius [72] in parentheses, in the 0–10% centrality bin. First panel of each set of three corresponds to $L_{\text{res}} = 0$, second one to $L_{\text{res}} = 2/(\pi T)$, and the third panel shows the goodness (χ^2 per degree of freedom) of each fit. The horizontal red (orange) lines show the 1σ (2σ) range of values of κ_{sc} obtained via a global fit to all nine LHC data sets, and the (almost indistinguishable) purple and green horizontal lines show the goodness of these global fits for $L_{\text{res}} = 0$ and $L_{\text{res}} = 2/(\pi T)$.
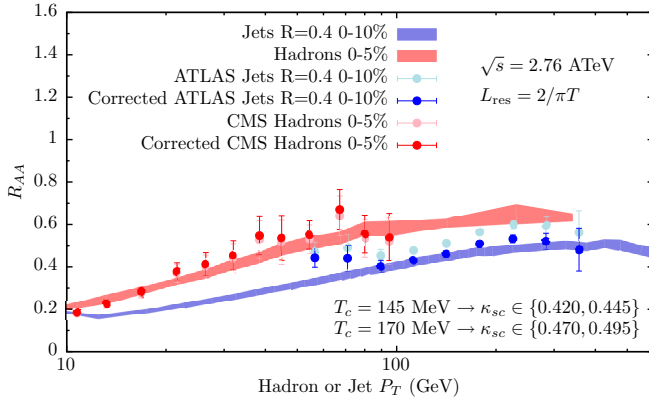
FIG. 2. Results for R_{AA}^{had} and R_{AA}^{jet} from our model with its pa-
rameter fixed via the global fit, compared to CMS [52] and ATLAS
[55] data. Error bars on the experimental data points show only the
uncorrelated error. The corrected data points (darker red and blue)
have been obtained from the uncorrected data points (paler red and
blue) by shifting them according to the best fit value of the correlated
error correction, obtained following the procedure from Ref. [61]
as detailed in the Supplemental Material [62]. Colored bands show
results from the hybrid model with $L_{res} = 2/(\pi T)$, with the bands
spanning results obtained with $T_c = 145$ and 170 MeV, in each case
using the one sigma range of values of κ_{sc} obtained from the global
fit in Fig. 1.

different sources of experimental uncertainty (statistical, un-
correlated systematic, correlated systematic, and normaliza-
tion) accounted for appropriately, as in Ref. [61]. We further
describe the fitting procedure in the Supplemental Material
[62] and provide an example in Fig. 2. Second, the horizontal
colored bands are obtained by performing a global fit to all
nine LHC data sets. The uncertainty bands on these global fits
correspond to the values of κ_{sc} for which $\chi^2 = \chi_{min}^2 \pm 1 (1\sigma)$
and $\chi^2 = \chi_{min}^2 \pm 4 (2\sigma)$. As in Refs. [11–14], increasing T_c or
increasing L_{res} without changing κ_{sc} reduces the quenching
of jets (and, here, of high-p_T hadrons) meaning that when
instead we fit the value of κ_{sc}, the value of κ_{sc} obtained from
the fit increases.

We conclude from the global fit that our model can simul-
taneously describe data on the suppression of both hadrons
and jets, yielding a satisfactory overall agreement between all
sets of LHC data within the narrow range for κ_{sc} indicated by
the global fit for either value of L_{res} and T_c. Although we cer-
tainly find no statistically significant preference for $L_{res} = 0$
or $L_{res} = 2/(\pi T)$ whatsoever, if we squint at Fig. 1 it appears
that the agreement between the band of values of κ_{sc} found via
the global fit and the jet suppression data looks slightly better
for $L_{res} = 2/(\pi T)$. The global fit shows that this impression
is not significant at present, but this impression—and the
goal of constraining the value of L_{res}—motivates future higher
statistics measurements of jet suppression. Note that although
at fixed κ_{sc} the effect of varying L_{res} on jet suppression is
significant, as noted in Ref. [63], this dependence becomes
rather weak after fitting the model parameter that controls
the rate of parton energy loss, in our case κ_{sc} which we
determine via our global fit. In any comparison between a

perturbative analysis and data, fitting the value of the jet-
quenching parameter $\hat{q}$ will have comparable consequences.

We see in Fig. 1 that the measurements of the suppression
of π^0 yields in RHIC collisions [61] favor a larger value of κ_{sc}
than the one we obtain from the global fit to LHC data, cor-
responding to a stronger coupling between energetic partons
and the QGP that they traverse in the lower temperature QGP
produced at RHIC. This is in line with the finding of previous
studies [64,65]. However, the distinction between the value
of κ_{sc} preferred for RHIC and LHC collisions is not at the
5σ level. This motivates future higher statistics measurements
of both hadron and jet suppression at RHIC. It would also
be interesting to extend this analysis to different centrality
classes.

Modification of jet fragmentation functions. Following the
discussion in the Introduction, we turn now to jet fragmen-
tation functions. By definition, fragmentation functions count
the mean number of hadrons, per jet, that carry a fraction z of
the whole jet energy, with z usually defined in experimental
analyses as $z \equiv (\mathbf{p}_h \cdot \mathbf{p}_j)/|\mathbf{p}_j|^2$, where $\mathbf{p}_h$ and $\mathbf{p}_j$ are the three-
momentum of the hadron and jet, respectively. The ratio
of fragmentation functions in PbPb and *pp* collisions was
introduced as an observable that is affected by jet quench-
ing in Ref. [66] and has been measured by both CMS and
ATLAS collaborations [66–68]. Here, we are interested in the
enhancement of this ratio close to $z \sim 1$. (The enhancement
in this ratio for soft particles with $p_T \lesssim 3$ GeV and hence
small z is of interest for reasons that are unrelated to our
considerations. This enhancement may receive a contribution
from loss of color coherence induced by multiple scatterings
with the medium [69,70]. And, assuming that the wake left
behind in the plasma by the jet becomes soft hadrons in this
momentum range, as is likely, which carry the momentum lost
by the jet, as is necessary by momentum conservation, then the
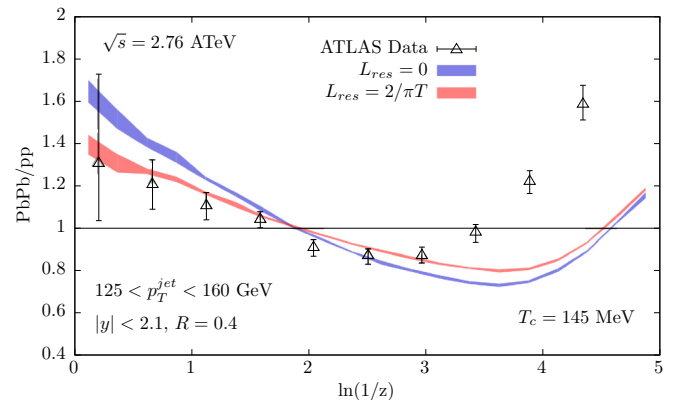wake must translate into an enhancement in the fragmentation

FIG. 3. The ratio of fragmentation functions for jets in PbPb
collisions with 125 GeV $< p_T^{jet} < 160$ GeV to those for jets with the
same p_T in pp collisions, with hybrid model predictions for $L_{res} = 0$
and $2/(\pi T)$ compared to ATLAS data [67]. In this observable,
we do see some evidence favoring $L_{res} = 2/\pi T$ over $L_{res} = 0$. The
disagreement between the hybrid model predictions and data at small
z, on the right, points to the need to improve the current hybrid model
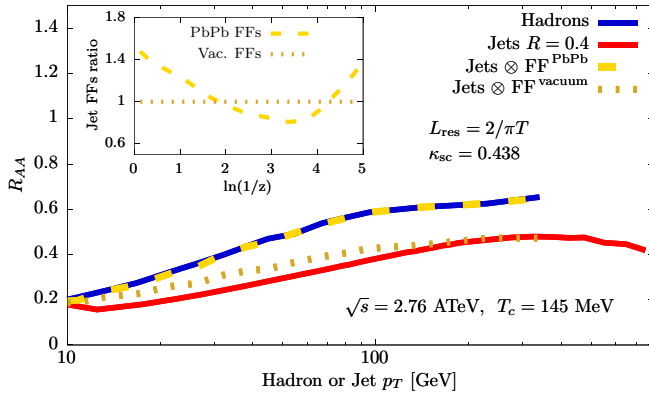implementation [13] of the wakes that jets deposit in the medium.

FIG. 4. Hybrid model results for R_{AA}^{had} (blue) and R_{AA}^{jet} (red) in LHC collisions with $\sqrt{s_{NN}} = 2.76$ TeV. The dashed yellow line shows the R_{AA}^{had} obtained by convolving the quenched jet spectrum with the hybrid model PbPb jet fragmentation function, shown in the inset. The dotted yellow line shows the R_{AA}^{had} obtained by convolving the quenched jet spectrum with an unmodified fragmentation function.

function ratio in this soft regime [13,71].) As we described in the Introduction, due to the steeply falling jet spectrum whenever we trigger on a high-p_T hadron we are biasing our sample toward narrow jets that fragmented into few, hard, hadrons. We see from the fragmentation function ratio near $z \approx 1$ in Fig. 3 that such jets are more common in PbPb collisions than in pp collisions. The agreement between our hybrid model calculations and these measured data suggests that this enhancement in the probability for finding hard fragmenting jets has the same origin as the lesser suppression of hadron yields relative to jet yields that our model also describes.

In Fig. 4, we show hybrid model calculations of R_{AA}^{had} and R_{AA}^{jet} for anti-k_t [72] radius $R = 0.4$, in collisions with $\sqrt{s_{NN}} = 2.76$ TeV with κ_{sc} set to its best fit value for $T_c = 145$ MeV and $L_{res} = 2/(\pi T)$, namely, $\kappa_{sc} = 0.438$. By convolving the PbPb (pp) jet spectrum with the appropriately binned fragmentation functions obtained in PbPb (pp) collisions whose ratio is depicted by the dashed yellow curve in the inset, one can recover the corresponding hadronic spectra and, in particular, the ratio of medium over vacuum spectra, as can be seen via the agreement between the dashed yellow curve in the main panel of Fig. 4 and the solid blue one. The most interesting comparison in Fig. 4 comes when we (incorrectly)

assume that the jet fragmentation function in PbPb collisions is the same as in pp collisions, as in the dotted yellow curve in the inset. We see that upon making this assumption we completely lose the ability to explain the difference between hadron and jet suppression, with the dotted yellow curve in the main panel showing that when the jet spectrum is convolved with this (incorrect) PbPb fragmentation function, the resulting (incorrect) hadron spectrum is rather similar to the jet spectrum. What we learn from this is that the difference between the suppression of hadron yields and jet yields, with $R_{AA}^{had} > R_{AA}^{jet}$ seen in experiments and in the hybrid model, is equivalent to the presence of a high-z enhancement in the fragmentation function ratio.

Conclusions. The enhancement in the ratio of fragmentation functions in PbPb and pp collisions at high-z was predicted using the hybrid strong-weak coupling model [13]. It originates from the fact that wider jets containing more partons at large angles on average lose more energy than narrower jets. This effect, together with the steeply falling jet spectrum, means that selecting a sample of jets with a given energy in PbPb collisions results in a bias toward finding narrow, hard fragmenting, jets. This mechanism enhances the fragmentation function at high z, as measured in experiments. Since when we select a sample of high-p_T hadrons we are selecting hadrons that come from unusually narrow jets with unusually hard fragmentation; the same effect also means that we are selecting hadrons from jets that lose less energy than typical jets do. Hence, hadron yields are less suppressed in PbPb collisions than jet yields are.

In support of these conclusions, we have seen that at the same time that the hybrid model provides a good description of the fragmentation function ratio at high z, it provides a simultaneous description of hadron and jet suppression in heavy-ion collisions.

[1] Y. Mehtar-Tani, J. G. Milhano, and K. Tywoniuk, Int. J. Mod. Phys. A **28**, 1340013 (2013).

[2] G. Y. Qin and X. N. Wang, Int. J. Mod. Phys. E **24**, 1530014 (2015).

[3] M. Connors, C. Nattrass, R. Reed, and S. Salur, Rev. Mod. Phys. **90**, 025005 (2018).

[4] W. Busza, K. Rajagopal, and W. van der Schee, Annu. Rev. Nucl. Part. Sci. **68**, 339 (2018).

[5] V. Khachatryan *et al.* (CMS Collaboration), J. High Energy Phys. 04 (2017) 039.

[6] The ATLAS Collaboration, ATLAS-CONF-2017-012 (unpublished).

[7] M. Aaboud *et al.* (ATLAS Collaboration), Phys. Lett. B **790**, 108 (2019).

[8] J. G. Milhano and K. C. Zapp, Eur. Phys. J. C **76**, 288 (2016).

[9] K. Rajagopal, A. V. Sadofyev, and W. van der Schee, Phys. Rev. Lett. **116**, 211603 (2016).

[10] J. Brewer, K. Rajagopal, A. Sadofyev, and W. Van Der Schee, J. High Energy Phys. 02 (2018) 015.

[11] J. Casalderrey-Solana, D. C. Gulhan, J. G. Milhano, D. Pablos, and K. Rajagopal, J. High Energy Phys. 10 (2014) 019; 09 (2015) 175.

[12] J. Casalderrey-Solana, D. C. Gulhan, J. G. Milhano, D. Pablos, and K. Rajagopal, J. High Energy Phys. 03 (2016) 053.

[13] J. Casalderrey-Solana, D. Gulhan, G. Milhano, D. Pablos, and K. Rajagopal, J. High Energy Phys. 03 (2017) 135.

[14] Z. Hulcher, D. Pablos, and K. Rajagopal, J. High Energy Phys. 03 (2018) 010.

[15] R. Baier, Y. L. Dokshitzer, A. H. Mueller, S. Peigne, and D. Schiff, Nucl. Phys. B **483**, 291 (1997).

[16] B. G. Zakharov, JETP Lett. **63**, 952 (1996).

[17] R. Baier, Y. L. Dokshitzer, A. H. Mueller, and D. Schiff, Nucl. Phys. B **531**, 403 (1998).

[18] M. Gyulassy, P. Levai, and I. Vitev, Nucl. Phys. B **594**, 371 (2001).

[19] U. A. Wiedemann, Nucl. Phys. B **588**, 303 (2000).

[20] X. N. Wang and X. F. Guo, Nucl. Phys. A **696**, 788 (2001).

[21] P. B. Arnold, G. D. Moore, and L. G. Yaffe, J. High Energy Phys. 06 (2002) 030.

[22] C. A. Salgado and U. A. Wiedemann, Phys. Rev. D **68**, 014008 (2003).

[23] S. Jeon and G. D. Moore, Phys. Rev. C **71**, 034901 (2005).

[24] P. Jacobs and X. N. Wang, Prog. Part. Nucl. Phys. **54**, 443 (2005).

[25] I. P. Lokhtin and A. M. Snigirev, Eur. Phys. J. C **45**, 211 (2006).

[26] J. Casalderrey-Solana and C. A. Salgado, Acta Phys. Polon. B **38**, 3731 (2007).

[27] K. Zapp, J. Stachel, and U. A. Wiedemann, Phys. Rev. Lett. **103**, 152302 (2009).

[28] K. Zapp, G. Ingelman, J. Rathsman, J. Stachel, and U. A. Wiedemann, Eur. Phys. J. C **60**, 617 (2009).

[29] I. P. Lokhtin, L. V. Malinina, S. V. Petrushanko, A. M. Snigirev, I. Arsene, and K. Tywoniuk, Comput. Phys. Commun. **180**, 779 (2009).

[30] N. Armesto, L. Cunqueiro, and C. A. Salgado, Eur. Phys. J. C **63**, 679 (2009).

[31] B. Schenke, C. Gale, and S. Jeon, Phys. Rev. C **80**, 054913 (2009).

[32] A. Majumder and M. Van Leeuwen, Prog. Part. Nucl. Phys. **66**, 41 (2011).

[33] J. Casalderrey-Solana, J. G. Milhano, and U. A. Wiedemann, J. Phys. G **38**, 035006 (2011).

[34] F. D'Eramo, M. Lekaveckas, H. Liu, and K. Rajagopal, J. High Energy Phys. 05 (2013) 031.

[35] X. N. Wang and Y. Zhu, Phys. Rev. Lett. **111**, 062301 (2013).

[36] K. C. Zapp, Eur. Phys. J. C **74**, 2762 (2014).

[37] J. Ghiglieri and D. Teaney, Int. J. Mod. Phys. E **24**, 1530013 (2015).

[38] Y. He, T. Luo, X. N. Wang, and Y. Zhu, Phys. Rev. C **91**, 054908 (2015); **97**, 019902(E) (2018).

[39] J. P. Blaizot and Y. Mehtar-Tani, Int. J. Mod. Phys. E **24**, 1530012 (2015).

[40] Y. T. Chien and I. Vitev, J. High Energy Phys. 05 (2016) 023.

[41] S. Cao *et al.* (JETSCAPE Collaboration), Phys. Rev. C **96**, 024909 (2017).

[42] F. Arleo, Phys. Rev. Lett. **119**, 062302 (2017).

[43] F. D'Eramo, K. Rajagopal, and Y. Yin, J. High Energy Phys. 01 (2019) 172.

[44] J. Casalderrey-Solana, H. Liu, D. Mateos, K. Rajagopal, and U. A. Wiedemann, *Gauge/String Duality, Hot QCD and Heavy Ion Collisions* (Cambridge University, Cambridge, UK, 2014).

[45] P. M. Chesler and K. Rajagopal, Phys. Rev. D **90**, 025033 (2014).

[46] P. M. Chesler and K. Rajagopal, J. High Energy Phys. 05 (2016) 098.

[47] Y. Mehtar-Tani, C. A. Salgado, and K. Tywoniuk, Phys. Lett. B **707**, 156 (2012).

[48] J. Casalderrey-Solana and E. Iancu, J. High Energy Phys. 08 (2011) 015.

[49] J. Casalderrey-Solana, Y. Mehtar-Tani, C. A. Salgado, and K. Tywoniuk, Phys. Lett. B **725**, 357 (2013).

[50] J. Casalderrey-Solana, D. Pablos, and K. Tywoniuk, J. High Energy Phys. 11 (2016) 174.

[51] J. Casalderrey-Solana and A. Ficnar, arXiv:1512.00371.

[52] S. Chatrchyan *et al.* (CMS Collaboration), Eur. Phys. J. C **72**, 1945 (2012).

[53] V. Khachatryan *et al.* (CMS Collaboration), Phys. Rev. C **96**, 015202 (2017).

[54] G. Aad *et al.* (ATLAS Collaboration), J. High Energy Phys. 09 (2015) 050.

[55] G. Aad *et al.* (ATLAS Collaboration), Phys. Rev. Lett. **114**, 072302 (2015).

[56] T. Sjostrand *et al.*, Comput. Phys. Commun. **191**, 159 (2015).

[57] K. J. Eskola, H. Paukkunen, and C. A. Salgado, J. High Energy Phys. 04 (2009) 065.

[58] J. Casalderrey-Solana, J. G. Milhano, and P. Quiroga-Arias, Phys. Lett. B **710**, 175 (2012).

[59] C. Shen, Z. Qiu, H. Song, J. Bernhard, S. Bass, and U. Heinz, Comput. Phys. Commun. **199**, 61 (2016).

[60] F. Cooper and G. Frye, Phys. Rev. D **10**, 186 (1974).

[61] A. Adare *et al.* (PHENIX Collaboration), Phys. Rev. Lett. **101**, 232301 (2008).

[62] See Supplemental Material at http://link.aps.org/supplemental/10.1103/PhysRevC.99.051901 for further details on the fitting procedure.

[63] Y. Mehtar-Tani and K. Tywoniuk, Phys. Rev. D **98**, 051501(R) (2008).

[64] W. A. Horowitz and M. Gyulassy, Nucl. Phys. A **872**, 265 (2011).

[65] C. Andrès, N. Armesto, M. Luzum, C. A. Salgado, and P. Zurita, Eur. Phys. J. C **76**, 475 (2016).

[66] S. Chatrchyan *et al.* (CMS Collaboration), Phys. Rev. C **90**, 024908 (2014).

[67] M. Aaboud *et al.* (ATLAS Collaboration), Eur. Phys. J. C **77**, 379 (2017).

[68] M. Aaboud *et al.* (ATLAS Collaboration), Phys. Rev. C **98**, 024908 (2008).

[69] Y. Mehtar-Tani and K. Tywoniuk, Phys. Lett. B **744**, 284 (2015).

[70] P. Caucal, E. Iancu, A. H. Mueller, and G. Soyez, Phys. Rev. Lett. **120**, 232001 (2018).

[71] W. Chen, S. Cao, T. Luo, L. G. Pang, and X. N. Wang, Phys. Lett. B **777**, 86 (2018).

[72] M. Cacciari, G. P. Salam, and G. Soyez, J. High Energy Phys. 04 (2008) 063.